Article:

Morley, N.A., Finkel, A.C., Yang, W. et al. (1 more author) (2014) Magnetic and structural characterization of NiFe/Fe30Co70 Bilayers. IEEE Transactions on Magnetics, 50 (11). 2503704. ISSN 0018-9464

https://doi.org/10.1109/TMAG.2014.2330001

Magnetic and Structural Characterisation of NiFe/$Fe_{30}Co_{70}$ bilayers

Nicola A. Morley, Member, IEEE, Anastasia Caruana Finkel, Weigang Yang and Nik Reeves-McLaren.

Abstract— Magnetostrictive films are required for a wide range of device applications; by increasing the magnetostriction constant and decreasing the anisotropy field, the devices will become more efficient. This paper has studied $Fe_{30}Co_{70}$ films on different thicknesses of the soft magnetic underlayer $Ni_{81}Fe_{19}$, to determine how the structural and magnetic properties change. It was found that the anisotropy field of the $Fe_{30}Co_{70}$ film could be reduced by 50% to 10kA/m and the magnetostriction constant increased by a factor 4 to 65ppm when grown on 30nm $Ni_{81}Fe_{19}$. This was due to the NiFe underlayer inducing a BCC(110) texture within the $Fe_{30}Co_{70}$ film and reducing the in-plane stress.

Index Terms—magnetostrictive films, MEMS, soft magnetic underlayers

I. Introduction

Magnetic microelectromechanical systems (MEMS) devices are being developed for a range of applications including magnetostrictive energy harvesters [1] and wireless mass sensors for detection of airborne toxins and water based nutrients [2]. To achieve the sensitivities required for these applications the magnetic films used must have a large magnetostriction constant (λ_s >50ppm) and a small anisotropy field (H_s <10kA/m) [1, 2]. Possible candidate materials for these applications include Fe-Co [3-6], Fe-Ga [7-9] and Metglas films [10].

Previous work by Hunter et al [3] showed that the magnetostriction constants of Fe-Co films could be as high as 250ppm, but strongly depended on fabrication procedure, which influenced the film microstructure. While the magnetostriction constants were high in these films, the anisotropy fields were also high i.e. H_s ~40kA/m for the quenched $Fe_{34}Co_{66}$ film. Similarly, work by Javed et al [7, 8] and Hattrick-Simpers et al [9] showed the magnetostriction constants for Fe-Ga films ranged from 50ppm to 150ppm depending on the fabrication method, but again the anisotropy fields were in general >50kA/m, with the lowest measured at 32 kA/m for a 50nm $Fe_{77}Ga_{23}$ film [7]. Both Fe-Co and Fe-Ga films would be ideal for the MEMS applications if the anisotropy field could be reduced. One method to achieve this, is to grow the films on thin underlayers, such as Cu, Rb, and NiFe. Jung et al [4] determined that Ta, Cu, NiFe and Ru underlayers strongly reduce the anisotropy field and coercive field of $Fe_{65}Co_{35}$ films by changing the film texture. Kotapati et al. [5] determined that when grown on a thicker NiFe underlayer, smaller anisotropy fields and larger magnetostriction constants can be achieved for 15nm $Fe_{50}Co_{50}$ films. Caruana Finkel et al. [6] also showed that increasing NiFe underlayer thickness led to smaller anisotropy fields in 25nm $Fe_{10}Co_{90}$ films; the magnetostriction constant could be tuned by varying NiFe thickness.

This work has studied 50nm $Fe_{30}Co_{70}$ films on soft magnetic underlayers, with the aim to achieve the large magnetostriction constants achieved by Hunter et al [3], in thinner films, but with anisotropy fields <10kA/m.

II. Experimental Procedure

Bilayer films were grown on cleaned silicon substrates with the native oxide layer still in place. The films were grown in a Nordiko RF sputterer, which had the capability for the soft magnetic underlayer and the $Fe_{30}Co_{70}$ film to be grown in sequence without exposing the underlayer to atmosphere. The soft magnetic underlayer was $Ni_{81}Fe_{19}$ (NiFe), grown at 4.8mTorr pressure and a power density of $1kW/m^2$, which was the lowest pressure and power for the system which allowed for uniform NiFe film growth [11]. The thickness of the NiFe films ranged from 0 to 30nm. The $Fe_{30}Co_{70}$ film was then deposited on top at 4.8mTorr pressure and a power density of $2kW/m^2$. The thickness of the $Fe_{30}Co_{70}$ films was 50nm. The thickness calibration of each layer deposited using the RF sputterer was checked before the bilayer growths, by measuring three monolith films of different thicknesses using an atomic force microscope. This ensured that the film thickness for each layer was ±1nm.

A Siemens D5000 diffractometer with a Cu K_α source (λ=1.5418Å) was used to collect the x-ray diffraction (XRD) patterns of the films. The XRD data were fitted in Fityk software package [12], to determine line position 2θ and full width at half maximum (FWHM) values. From these measured

This paragraph of the first footnote will contain the date on which you submitted your paper for review.

N. A. Morley, Department of Materials Science and Engineering, University of Sheffield, Sheffield, S1 3JD (e-mail: n.a.morley@sheffield.ac.uk).

A. Caruana Finkel, Department of Materials Science and Engineering, University of Sheffield, Sheffield, S1 3JD (e-mail: anastasia.finkel@gmail.com)

W. Yang, Department of Materials Science and Engineering, University of Sheffield, Sheffield, S1 3JD (e-mail: mtp12wy@sheffield.ac.uk)

N. Reeves-McLaren, Department of Materials Science and Engineering, University of Sheffield, Sheffield, S1 3JD (e-mail: n.reeves@sheffield.ac.uk)

values, the lattice constant (a) was determined using Bragg's law, along with the homogenous strain (ε) and stress (σ) [13]. The minimum grain size (D) was determined from the XRD data using the Scherrer equation [13]. The magnetic properties were measured on a Magneto-optic Kerr Effect (MOKE) magnetometer [6-8]. From the normalised hysteresis loops, the anisotropy fields (H_s) and coercive fields (H_c) were determined, while the anisotropy was inferred from the normalised remanent magnetisation. The effective magnetostriction constant (λ_{eff}) was determined using the Villari Effect technique [6-8]. This involves bending the film along the hard axis over a known bend radius within a MOKE magnetometer. The change in anisotropy field as a function of bend radii (R) is then plotted (Fig. 3a), and the effective magnetostriction constant determined using the equation:

$$\lambda_{eff} = \frac{dH_S}{d^1/_R}\frac{\mu_o M_S E}{3\upsilon\tau} \qquad (1)$$

Where $\mu_o M_s$ is saturation magnetization (2.2T for $Fe_{30}Co_{70}$), υ is the Poisson ratio of the substrate, E is the Young's Modulus of the substrate and τ is the substrate thickness. The values of the Poisson ratio and Young's modulus of the 380µm silicon substrate are known from the literature [14]. The saturation magnetization of the 50nm $Fe_{30}Co_{70}$ films is assumed to be the same as bulk $Fe_{30}Co_{70}$, as previous work on thin films found that the magnetization was reduced from the bulk value for films thinner than 2.5nm [15], thus at 50nm the saturation magnetization can be taken as the bulk value.

III. Results and Discussion

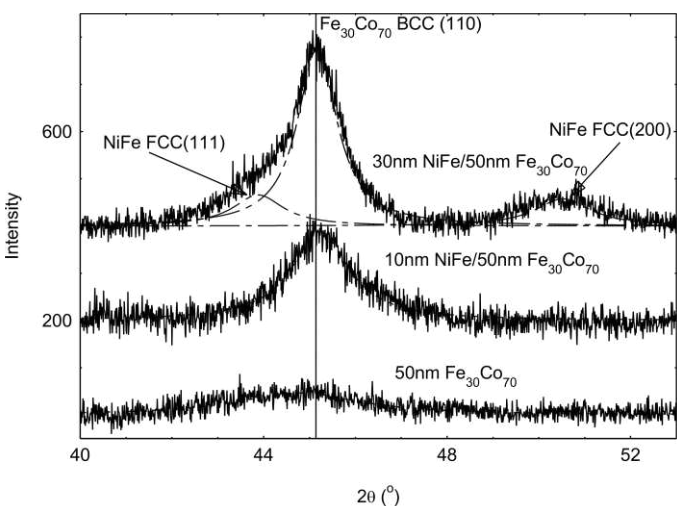

Fig. 1. XRD data for the 50nm $Fe_{30}Co_{70}$ films grown on NiFe underlayers. The dashed lines are a fit to the data.

XRD data, Fig. 1, showed a peak at $2\theta \sim 45^o$, for all three $Fe_{30}Co_{70}$ films, which increasing in sharpness with NiFe layer thickness. This peak is attributed to the BCC(110) peak, which occurs at $2\theta = 45.14^o$ for bulk $Fe_{30}Co_{70}$ (solid line in Fig. 1). The peaks were fitted using Fityk [12], and this fitting is plotted as dashed lines in Fig. 1. For the 30nm NiFe/50nm $Fe_{30}Co_{70}$ film, two extra peaks are observed in the data along with the expected BCC(110) peak. These peaks are attributed to the NiFe underlayer and are the FCC (111) peak at 43.87° and the FCC(200) peak at 50.52°. As the BCC(110) peak increases in sharpness with NiFe thickness, this means that growing on the NiFe underlayer has improved the texture within the $Fe_{30}Co_{70}$ film. For the $Fe_{30}Co_{70}$ film grown with no underlayer, XRD data shows no preferred texture within the film, with all textures as likely. For the $Fe_{30}Co_{70}$ films grown on a NiFe underlayer, the NiFe has caused the BCC(110) direction in the $Fe_{30}Co_{70}$ films to become aligned perpendicular to the substrate, thus providing the $Fe_{30}Co_{70}$ films with a strong texture direction within it.

TABLE I
Summary of the Lattice Constants, Strains, Stresses and Grain Size for the $Fe_{30}Co_{70}$ Films

Film	Lattice constant, a (Å)	Strain, ε	Stress, σ (GPa)	Grain Size, D (nm)
50nm $Fe_{30}Co_{70}$	2.86 ± 0.03	-	-	3 ± 1
10nm NiFe/ 50nm $Fe_{30}Co_{70}$	2.831± 0.004	-0.0021 ± 2×10^{-5}	1.42 ± 0.01	7 ± 0.5
30nm NiFe/ 50nm $Fe_{30}Co_{70}$	2.836 ± 0.004	-0.0004 ± 1×10^{-5}	0.24 ± 0.01	10 ± 0.5

The lattice constant, grain size, homogenous strain and stress for each film are given in table 1. For the 50nm $Fe_{30}Co_{70}$ film grown with no underlayer, the lattice constant is larger than the bulk $Fe_{30}Co_{70}$ lattice constant (a_o = 2.837Å), suggesting there is a small compressive stress within the film. Due to the broad width of the peak and the low signal to noise ratio (SNR = 4), the error on the lattice constant is larger than the bilayer films. This means that although the fitted peak 2θ is smaller than the bulk value, the large error on it means that it is within error of the bulk value. Thus no strain and stress values are given, due to the large uncertainty in the data. For the $Fe_{30}Co_{70}$ films grown on NiFe, the lattice constants are smaller than the bulk constant, though within errors, suggesting a small in-plane tensile stress within the film. The in-plane stress is also a factor 6 smaller in the 30nm NiFe/50nm $Fe_{30}Co_{70}$ film compared to the 10nm NiFe/50nm $Fe_{30}Co_{70}$ film. This means growing $Fe_{30}Co_{70}$ films on NiFe films has changed both overall texture within the film and in-plane stress. The growth on NiFe has also affected the grain size within the $Fe_{30}Co_{70}$ films. The grain size was determined using the Scherrer equation [13], which depends on the 2θ peak as well as the full width at half maximum (FWHM) of the XRD peak. Thus again due to the SNR and broad peak width of the 50nm $Fe_{30}Co_{70}$ film with no underlayer, the grain size quoted is a minimum value, as the grain size increases with decreasing FWHM. Therefore the data suggests that the 50nm $Fe_{30}Co_{70}$ film with no underlayer had a grain size of 3nm, while for the 30nm NiFe/50nm $Fe_{30}Co_{70}$ film the grain size had increased to 10nm, which will in part be to be due to the BCC(110) texture in the film, improving the FWHM of the XRD peak.

From Fig. 2, it is observed that the shape of the hard axis magnetisation loop changes as the thickness of the NiFe underlayer thickness increases. The anisotropy field decreases by 50%, from 20±2 kA/m for the $Fe_{30}Co_{70}$ film to 10±2 kA/m for the 30nm NiFe/50nm $Fe_{30}Co_{70}$ film. This will be due to the NiFe underlayer, which has reduced the stress and increased the BCC(110) texture in the films. This is because the anisotropy field is directly proportional to the stress in the film [16], thus a decrease in the in-plane stress, will reduce the anisotropy field of the film, as observed in Fig.2.

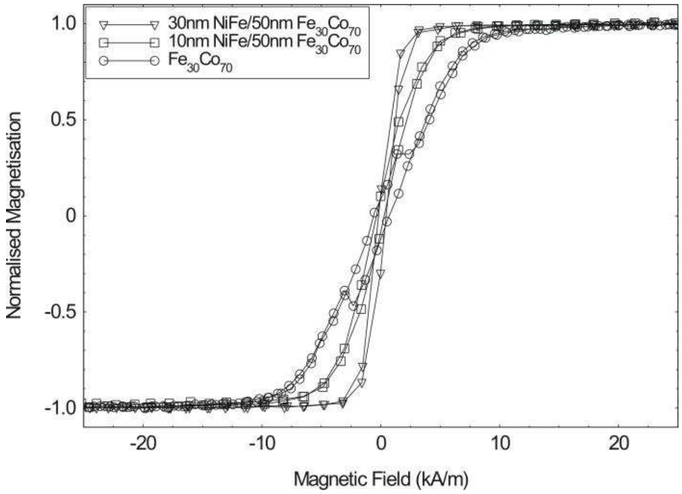

Fig. 2. Normalised hard axis magnetisation loops as a function of magnetic field for the 50nm $Fe_{30}Co_{70}$ films grown on NiFe underlayers

From Fig. 2, the coercive field reduces by a half as well, from 0.7±0.2 kA/m for the $Fe_{30}Co_{70}$ film to 0.35±0.2 kA/m for the 10nmNiFe/50nm $Fe_{30}Co_{70}$ film. The coercive field depends on the microstructure and grain size within the film [4]. For $Fe_{30}Co_{70}$ films, the film structure went from no defined texture for the $Fe_{30}Co_{70}$ film to strong BCC(110) texture for the $Fe_{30}Co_{70}$ films grown on NiFe; this change in microstructure will be the cause for the reduction in the H_c. Although the anisotropy fields and coercive fields were reduced when growing on NiFe underlayers, the overall uniaxial anisotropy within the films was maintained.

The effective magnetostriction constants of the $Fe_{30}Co_{70}$ films were measured using the Villari Effect (eqn (1)) and are plotted in Fig. 3b, along with the change in anisotropy field as a function of inverse bend radii (Fig. 3a). For the 50nm $Fe_{30}Co_{70}$ film with no underlayer, the effective magnetostriction constant was +17±4ppm, while for the 10nm NiFe/50nm $Fe_{30}Co_{70}$ the effective magnetostriction constant was +14±4ppm, therefore within error of the monolith film. Thus growing on the thin NiFe layer did not effect the overall effective magnetostriction constant. The slight decrease in effective magnetostriction constant could be due to the effective magnetostriction constant of 10nm NiFe on silicon being -2.25ppm [17]. For the 30nm NiFe/50nm $Fe_{30}Co_{70}$, the effective magnetostriction constant was +65±4ppm, thus growing on the thicker NiFe film has increased the effective magnetostriction constant to larger than the bulk polycrystalline value (~57ppm [18]). A similar effect was observed in the effective magnetostriction constants of 15nm $Fe_{50}Co_{50}$ films [5] grown on NiFe underlayers. Hunter et al [3] measured the effective magnetostriction constants of 500nm $Fe_{30}Co_{70}$ films, for different processing methods. The values they achieved were λ_{eff} = ~75ppm for the as grown films, λ_{eff} = ~140ppm for the slow cooled films and λ_{eff} = ~250ppm for the quenched films. The texture and phases in the films changed with the different processed, which shows that the effective magnetostriction constant is strongly linked to the film structure. For the 30nm NiFe/50nm $Fe_{30}Co_{70}$ film, the effective magnetostriction constant is in agreement with Hunter's as-grown films value.

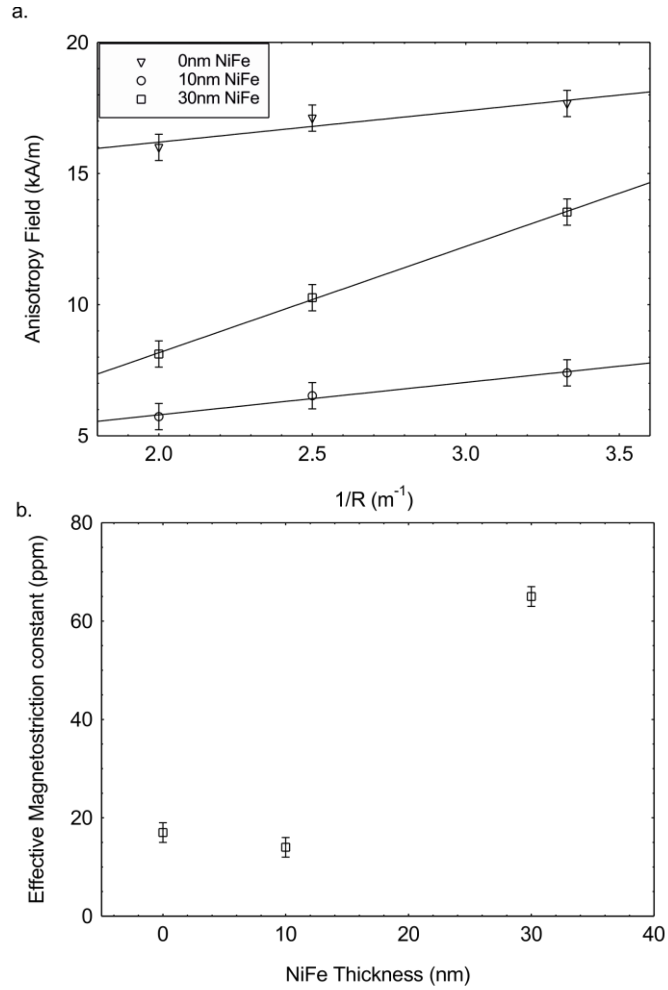

Fig 3a. Anisotropy field as a function of inverse bend radii for the $Fe_{30}Co_{70}$ films Fig. 3b. Effective magnetostriction constants as a function of NiFe thickness for $Fe_{30}Co_{70}$ films.

From Hunter et al [3] work, the increase in the effective magnetostiction constant is likely to be due to two effects, the first the changing of texture from randomly orientated to (110) texture and the second is the reduction in stress in the $Fe_{30}Co_{70}$ films. For a randomly orientated polycrystalline film, such as the 50nm $Fe_{30}Co_{70}$ film without an underlayer, the effective magnetostriction constant is given by [19]:

$$\lambda_{isotropic} = \frac{2}{5}\lambda_{100} + \frac{3}{5}\lambda_{111} \qquad (2)$$

Where λ_{100} is the magnetostriction constant along the (100) direction and λ_{111} is the magnetostriction constant along the (111) direction. While for a textured (110) film, such as the 30nm NiFe/50nm $Fe_{30}Co_{70}$ film the effective magnetostriction constant is given by [19]:

$$\lambda_{(110)} = \frac{1}{5}\lambda_{100} + \frac{4}{5}\lambda_{111} \qquad (3)$$

Thus both effective magnetostriction constants depend differently on the λ_{100} and λ_{111} values. For bulk $Fe_{30}Co_{70}$, the values of λ_{100} and λ_{111} have not been published, with Hall [20] only measuring λ_{100} and λ_{111} up to 60%Co in Fe. Bozorth [18] presented effective magnetostriction constants for bulk $Fe_{30}Co_{70}$ polycrystalline samples, with the largest value being

130ppm for a hard rolled tape, which had oriented domains compared to 57ppm for bulk polycrystalline samples. Therefore the difference in the effective magnetostriction constants between the 50nm $Fe_{30}Co_{70}$ film and the 30nm NiFe/50nm $Fe_{30}Co_{70}$ film could arise from the change in texture in the films.

The effective magnetostriction constant is also influenced by the stress in the film and can be predicted by [16]: $\lambda_{net} = \frac{\mu_o M_s H_s}{3\sigma}$, where $\mu_o M_s$ is the saturation magnetisation (for $Fe_{30}Co_{70}$ films is 2.2T), H_s is the anisotropy field and σ is the in-plane stress. Putting the variables in for the films grown on NiFe underlayers, as the XRD peak for the 50nm $Fe_{30}Co_{70}$ film with no underlayer (Fig. 1) was too broad to determine a stress for the film, gives λ_{net} = 2.5ppm for the 10nm NiFe/50nm $Fe_{30}Co_{70}$ film and λ_{net} = 31ppm for the 30nm NiFe/50nm $Fe_{30}Co_{70}$ film. Although they are smaller than the measured effective magnetostriction constants, there is a large difference between the 10nm NFe/50nm $Fe_{30}Co_{70}$ film and the 30nm NiFe/50nm $Fe_{30}Co_{70}$ film effective magnetostriction constants. Thus showing that changes in stress in the films lead to the large change in the effective magnetostriction constant. This suggests that the large effective magnetostriction constant measured for the 30nm NiFe/50nm $Fe_{30}Co_{70}$ film is due to both the reduction in stress and increase in the BCC(110) texture in the film.

IV. Conclusions

Growing $Fe_{30}Co_{70}$ films on thin NiFe underlayers has improved the magnetic properties of the $Fe_{30}Co_{70}$ films, such that they could be considered for MEMS applications. For example growing the 50nm $Fe_{30}Co_{70}$ film on a 30nm NiFe underlayer, reduced the anisotropy field by 50% to 10kA/m, while the effective magnetostriction constant increased to 65ppm. From XRD data, the $Fe_{30}Co_{70}$ films grown on NiFe underlayers had strong BCC(110) texture within the film compared against the $Fe_{30}Co_{70}$ film grown with no underlayer. Growing $Fe_{30}Co_{70}$ films on NiFe improved the film texture in the films, with a concomitant reduction in the anisotropy fields and increased effective magnetostriction constant.

References

[1] O. Gutfleisch, M. A. Willard, W. E. Bruck, C. H. Chen, S. G. Sanker, and J. Ping Liu, "Magnetic Materials and Devices for the 21st Century: Stronger Lighter and More Energy Efficient," Adv. Mats, vol. 23, pp. 821-842, 2011.

[2] M. R. J. Gibbs, E. W. Hill, and P. J. Wright, "Magnetic materials for MEMS applications," J. Phys D: Appl. Phys, vol. 37, pp. R237 - R244, 2004.

[3] D. Hunter, W. Osborn, K. Wang, N. Kazantseva, J. Hattrick-Simpers, R. Suchoski, R. Takahashi, M. L. Young, A. Mehta, L. A. Bendersky, S. E. Lofland, M. Wuttig, and I. Takeuchi, "Giant Magnetostriction in annealed CoFe thin-films," Nat. Commun, vol. 1529, pp. 1 - 7, 2011.

[4] H. S. Jung, W. D. Doyle, and S. Matsunuma, "Influence of underlayers on the soft properties of high magnetisation FeCo films," J. Appl. Phys, vol. 93, pp. 6462 - 6464, 2003.

[5] S. Kotapati, A. Javed, N Reeves-McLaren, M. R. J. Gibbs and N. A. Morley, "Effect of the NiFe thickness on the magnetic properties of NiFe/FeCo bilayers", J. Magn. Magn. Mats, vol. 331, pp 67-71, 2013

[6] A. Caruana Finkel, N. Reeves-McLaren and N. A. Morley, "Influence of soft magnetic underlayers on the magnetic properties of $Co_{90}Fe_{10}$ films" J.Magn. Magn. Mats, vol. 357, pp 87-92, 2014

[7] A. Javed, T. Szumiata, N. A. Morley, and M. R. J. Gibbs, "An investigation of the effect of structural order on magnetostriction and magnetic behaviour of Fe-Ga thin films," Acta Mat, vol. 58, pp. 4003, 2010.

[8] A. Javed, N. A. Morley, and M. R. J. Gibbs, "Structure, Magnetic and Magnetostrictive Properties of as-deposited Fe-Ga Thin Films," J. Magn. Magn. Mats, vol. 321, pp. 2877, 2008.

[9] J. R. Hattrick-Simpers, D. Hunter, C. M. Craciunescu, K. S. Jang, M. Murakami, J. Cullen, M. Wuttig, I. Takeuchi, S. E. Lofland, L. Benderksy, N. Woo, R. B. Van Dover, T. Takahashi, and Y. Furuya, "Combinatorial investigation of magnetostriction in Fe-Ga and Fe-Ga-Al," Appl. Phys. Letts, vol. 93, pp. 102507, 2008.

[10] H. Szymczak and R. Zuberek, " Models of stress-induced anisotropy and magnetostriction in metallic glasses", IEEE Trans Magn, vol. 26, pp. 2551-2553, 1987

[11] A. V. Svalov, I. R. Aseguinolaza, A. Garcia-Arribas, I. Orue, J. M. Barandiaran, J. Alonso, M. L. Fernandez-Gubieda and G. V. Kurlyandskaya, "Structure and Magnetic Properties of Thin Permalloy Films near the "Transcritical" state", IEEE. Trans. Mag, vol. 46, pp. 333-336, 2010

[12] M. Wojdyr, "Fityk: a general purpose peak fitting programme," J. Appl. Crystall, vol. 43, pp. 1126-1128, 2010.

[13] C. Hammond, "The Basics of Crystallography and Diffraction", 3rd ed. Oxford: Oxford University Press, 2009

[14] D. R. Franca and A. Blouin, "All-optical measurement of in-plane and out-of-plane Young's modulus and Poisson's ratio in silicon wafers by means of vibration modes", Meas. Sci. Technol. Vol 15, pp. 859-868, 2004

[15] C. A. Neugebauer, "Saturation Magnetisation of Nickel Films of Thickness less than 100A", Phys. Rev. Vol 116, pp1441-1446, 1959

[16] N. A. Morley, S. Rigby, and M. R. J. Gibbs, "Anisotropy and magnetostriction constants of nanostructured FeCo films," J. Optoelec Adv. Mats, vol. 1, pp. 109 - 113, 2009.

[17] M. P. Hollingworth, M. R. J. Gibbs and S. J. Murdoch, "Magnetostriction and surface roughness of ultrathin NiFe films

[18] R.M. Bozorth, "Ferromagnetism", IEEE Press, New York, 1978

[19] A. Javed, N. A. Morley, T. Szumiata and M. R. J. Gibbs, "A comparative study of the microstructural and magnetic properties of <110> textured thin polycrystalline $Fe_{100-x}Ga_x$ ($10 < x < 35$) films", Appl. Surf. Sci, vol. 257, pp. 5977 – 5983, 2011

[20] R. C. Hall, "Magnetic Anisotropy and Mgnetostriction of Ordered and Disordered Cobalt-Iron Alloys", J. Appl. Phys. Vol 31, pp 157S – 158S 1960